Parametric Modeling of the Beating Heart with Respiratory Motion Extracted from Magnetic Resonance Images

G Pons Moll[1], G Crosas Cano[2], G Tadmor[3], RS MacLeod[4],
B Rosenhahn[1], DH Brooks[3]

[1]Leibniz Universitat /Institut fur Informationsverarbeitung (TNT),Hannover, Germany
[2]Technical University of Catalonia, Barcelona, Spain
[3]ECE Department, Northeastern University, Boston, MA, USA
[4]CardioVascular Research and Training Institute, University of Utah, Salt Lake City, UT, USA

Abstract

In atrial fibrillation ablation procedures on-line measurement of catheter position is often displayed to the clinician against a static anatomy from pre-procedure scans. However the heart is moving due to both contraction and respiratory motion. Thus both small-scale and large-scale inaccuracies are introduced into the visualization. As part of a larger project to improve delivery of ablation, we are developing parametric models to animate static three-dimensional pre-procedure anatomical models to include the dynamics. To make our heart model "beat" we combine image processing methods with Fourier and polynomial representations, and combine global and local smoothing. The result is an efficient parameterization of the moving surface over both space and time. The steps for making the heart move due to respiration are only partially complete. Here we concentrate on registering a sequence of ungated MR slice sequences. The approach involves parameterizing motion of curves representing anatomical landmarks and enforcing consistency in the cross-slice direction.

1. Introduction

In catheter-based fibrillation ablation procedures on-line measurement of catheter position, e.g. through magneto-tracking devices, is often displayed to the clinician against a static anatomy resulting from pre-procedure scans. However real-time localization of the catheter is in laboratory rather than anatomical coordinates. Typically a static registration of a representation of the anatomy during the procedure to the pre-procedure images is done at the outset, and then the on-going imaging of catheter position is visualized against that background. However, the heart is obviously moving during the procedure, primarily due to both contraction/dilation and thoracic respiration [1]. As a result both small-scale (beating) and large-scale (respiratory) inaccuracies are introduced into the on-line representation, which can decrease the clinician's ability to confidently navigate the anatomy during the procedure.

As a contribution to a larger project on image-based approaches to atrial fibrillation at the University of Utah, we have been developing parametric models for use in animating a static three-dimensional pre-procedure anatomical model to enable representation of the on-going dynamics, *i.e.* to build a dynamic, 4D heart model. The eventual goal is to be able to update the pre-procedure model with whatever data is available, including 2D MR scans, intracavitary echocardiography (ICE), fluoroscopy, etc. We have divided this project into two steps: building a 4D parametric model of the beating heart, and building a 4D parametric model of the heart moving under respiration. We report here on the approach to the first step and some first steps towards the second. The basis for both approaches were series of 2D MR scans in controlled settings. However there are some inherent difficulties in obtaining adequate data for both modeling scenarios, and we discuss these concerns below.

The problem of automatic cardiac segmentation has been extensively investigated. Numerous methods in the literature rely on previous learning of the shape and appearance of cardiac structures from training examples [2–4]. These algorithms can encode higher level knowledge about the appearance and shape of the heart and are hence can be quite robust. The main concerns related to these models are data collection and manual segmentation and registration of the training samples, as this training process is usually very time consuming. Non-parametric evolving curves like level sets [5] have also been used for

segmentation of cardiac volumes. However, level set based methods are computationally very expensive and the behavior of the evolving interface is difficult to control without any shape prior [6, 7]. We note that the well-known ability of level sets to naturally handle topological changes is not particularly useful for the application at hand.

2. Methods

In the first part of our work, we propose an efficient pipeline for the automatic segmentation and tracking of the epicardium and left ventricle from (respiration-gated) MRI cine sequences of the heart. Our active contour [8] based method does not require a model learned from a database. Compared to other methods to segment cardiac contours, our method offers the following potential advantages:
1. The heart is quickly localized based on the distinctive time variance of the heart region. In contrast to other methods that detect the heart in single images [9, 10], our method detects the whole heart volume giving spatial consistency to the initialization.
2. Temporal and spatial consistency is jointly enforced in the segmentation by fitting an m-tensor smoothing spline to the radial functions of the time-surfaces.
3. Our heart localization method can be easily integrated in Appearance and Shape Model based approaches to initialize the position and orientation of the model. Moreover, methods based on Active Contours and Deformable Models can benefit from the time-space consistency.
Our overall heart localization and segmentation framework is outlined in the flow chart in Fig. 1.

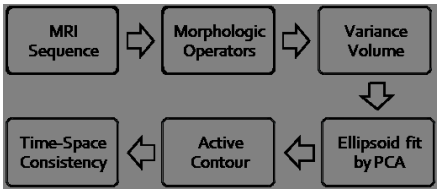

Figure 1. The flow chart to model heart beat motion

In the first stage, we roughly localize the heart volume by finding the bounding ellipsoid that encloses the heart in all the cardiac phases. In the second stage, with this initial curve we find the border of the heart by means of energy minimization. The resulting segmented cardiac volume is propagated to the next frame and the algorithm is iterated until the segmentations for all the cardiac phases are obtained. In a final stage, time and space consistency is enforced in the planar segmentations by fitting an m-tensor smoothing spline to all time surfaces in a single optimization step.

In the second part of our work, we report on initial work modeling the motion of the heart under respiration. We note that it is not straightforward to acquire adequate MR data for this task, as synchronization between adjacent slices is not available (at least in our study where we did not have access to an auxiliary position signal), joint ECG and respiratory gating is difficult and requires very long recording times, ECG gating causes overly sparse sampling of the respiratory cycle, and adequate coverage and sampling to allow imposition of joint models from both saggital and axial planes is a challenge [11]. We were able to achieve some success through the use of ungated data along with a navigator signal which we used to extract respiratory phase.

The main steps of the method are:
1. Extract respiratory phase for each image from the navigator signal
2. Find the boundary of the heart in every image
3. Interpolate to a regular sampling of respiratory phase
4. Create an averaged heart at each chosen phase sample
5. Extract respiratory motion as translation and rotation using the centroids and the averaged hearts

2.1. 4D modeling of the beating heart

2.1.1. Pre-processing and initialization

To filter noise in the MRI slices and remove nearby vessels we perform a morphological opening followed by masking with binary image created from the opened image by thresholding. Next we initialize our model of the heart by looking for pixels with large temporal variance. Specifically we compute the time variance volume V_σ:

$$V_\sigma = \frac{1}{T}\sum_{t=1}^{T}(V_t - V_\mu)^2 \quad \text{where} \quad \mathrm{V}_\mu = \frac{1}{\mathrm{T}}\sum_{\mathrm{t}=1}^{\mathrm{T}}\mathrm{V}_\mathrm{t}. \qquad (1)$$

We then binarize V_σ and find the largest connected region. The threshold is selected so that as many pixels as the heart volume are preserved. In order to initialize our active contour we find the minimum enclosing ellipsoid by Principal Component Analysis. This provides an initial estimate of the volume for the first frame.

2.1.2. Segmentation

For segmentation we evolve an active contour parametrized with Fourier coefficients. For each slice in the MRI volume we use the cross-sections of the initialization ellipsoid as the initial estimates for our active contour. The segmented volume for the current time frame is used as the initialization for the next frame. The boundary of the epicardium is found by moving every point in the curve in the radial

direction to minimize the energy functional

$$\mathrm{argmin}_{\mathbf{x}\in\mathrm{Window}}\mathrm{w}_1\frac{\mathrm{d}^2\mathrm{u}}{\mathrm{d}\mathbf{x^2}} - \mathrm{w}_2\langle\nabla\mathrm{I}(\mathbf{x}),\vec{r}(\theta_\mathbf{i})\rangle - \mathbf{w_3 u} \quad (2)$$
$$-w_4|r(\theta_{i-1}) - r(\mathbf{x},\theta_\mathbf{i})|$$

where $\mathbf{x} = [\mathbf{x},\mathbf{y}]^\mathbf{T}$ denotes the image locations in the search window, u is the image intensity curve in the radial direction, $\nabla I(\mathbf{x})$ is the image gradient found using Sobel filters in the horizontal and vertical directions, $r(\mathbf{x},\theta_{\mathbf{i-1}})$ is the radius of the candidate with respect to the centroid and $r(\theta_{i-1})$ is the radius of the previous candidate minimizer in the curve. To avoid mesh resampling we first resampled the curve every 5 degrees and then, for each point, chose the location that minimizes Eq. (2).

2.1.3. Enforcing time and space consistency

For each frame we have now obtained a set of planar contours with cylindrical topology. However the resulting surfaces were not smooth and in particular showed considerable jitter in time. In order to enforce greater spatio-temporal consistency, we further refined the segmentation by fitting it with an m-tensor smoothing spline across both 3-space and time in a single optimization step. We found that this sort of local optimization method was more suited for the problem at hand than global methods such as 3D Fourier descriptors. Specifically, we constructed a tensor Θ of order 3 from the radii of the time-space curves preserving the topology. Columns of the tensor were formed by the radial functions of the planar contours in a given time and slice location. Therefore, each element $(R(\theta,z,t))$ of the tensor Θ was approximated by

$$R(\theta,z,t) = f(\theta)g(z)h(t) \quad (3)$$

where $f(\theta), g(z), h(t)$ are uni-variate splines that enforce consistency in each of the 3 dimensions involved: within the same contour, across the slices, and in time, respectively. We chose piecewise cubic polynomial functions with constraint equations $f(x)$ to approximate our points. The function $f(x)$ minimizes:

$$p\sum_{j=1}^{N} w_j|y(j) - f(j)|^2 + (1-p)\int |f''(x)|^2\,dx \quad (4)$$

The choice of p controls a tradeoff between accuracy and smoothing. Besides this constraint we impose that $f(x)$ is twice differentiable, $f(x) \in C^2$. This gives rise to three additional equations for each data site. Combining these equations with equations in (4) we generated a linear system $Ax = b$ and solved in a least squares fashion to find the vector of polynomial coefficients. For a more detailed explanation on the pipeline to model the heart beat we refer to [12]

2.2. Modeling the heart under respiration

We model the motion of the heart due to respiration as rigid body motion, i.e. we retrieve only rotation and translation. As noted above we used ungated MR sequences along with a navigator signal. Since the aquisition was unsynchronized for the different cross-sections of the heart (i.e. in a given frame, adjacent slices are essentially randomly sampled in terms of respiratory phases) the first step is to synchronize the data using the navigator signal [13]. The navigator signal measures the position of an anatomical landmark (the liver or diaphragm) during free breathing aquisition (Fig 2.2). Automatically extracting the navigator reflection and normalizing all respiratory cycles to a common maximum excursion in both directions, we can assign a normalized phase point to each slice. Sampling the respiratory cycle at ten equally-spaced phase points, we associate each the slice with one of those phase samples. Thus we obtain multiple cross-sections of the heart at each respiratory phase. Note that the number of times we observe a given slice of the heart in the same phase depends on the uncontrolled relationship between respiration and acquisition timing of that slice, and therefore the number of observations of phases is in general diferent for every cross-section. Next we find the heart border for every

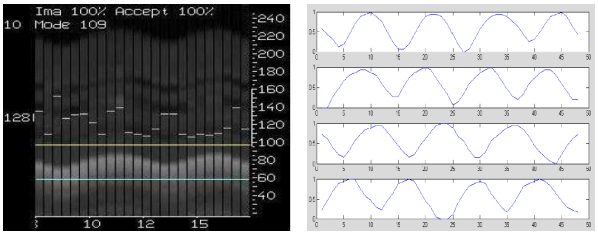

Figure 2. Navigator signal on the right, Reconstructed respiratory cycles on the left

available image, similarly to our work modeling the beating heart. However, we are limited to 2-D, not volume, segmentation because we are working with free breathing acquisition, and some volumes might be incomplete for a given phase. Grouping these 2D contours according to their assigned respiratory phase, we obtain samples of ten volumes, one at each phase sample. Of course each slice may be at different phase point of the contraction cycle. Assuming that we have enough samples to smooth out that higher-frequency motion, we average all the contour samples of a given phase. The result is ten heart surfaces, one for each sampled phase point. From these surfaces, extraction of rotation and translation is straightforward. We measure translation by calculating and then substracting the centroids of consecutive volumes, and rotation by simply finding the best match between the model volume and multiple possible rotations.

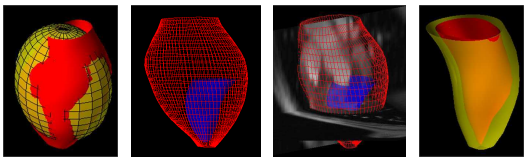

Figure 3. From left to right: Initial ellipsoid localization in yellow overlapped with the final segmentation, Epi volume with the LV inside; Segmentation with the long axis cross-section, LV during end-systole and end-dyastole

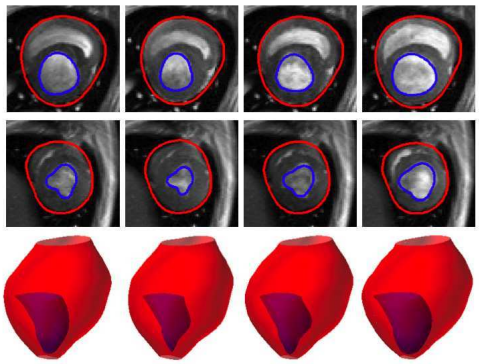

Figure 4. **Epi and LV surfaces and contours**-Result of the segmentation for different slices 9 and 15 in the vertical direction. The cardiac phases correspond to mid-systole, end-systole, mid-dyastole, end-dyastole

3. Results

For the contraction modeling we have conducted experiments on two 4D canine cardiac MRI datasets, each with 12 cardiac phases with 20 Short Axis (SA) cross-sections per phase. We show the resulting segmented epicardial and left ventricular surfaces in Figs. 4 and 3. In Fig. 3(c) we show how the (Epi) surface, in red, and the (LV) surface in blue, fit the cardiac volume.

For the respiratory modeling, Fig. 5, we show on the left contours of all slices assigned to a given phase sample, along with the averaged contour calculated from those samples. On the right we show the centroid trajectory calculated from the averaged hearts at all phase samples. We note that the respiratory motion trajectory is reasonable when compared to the original images, but appears to underestimate the extent of the motion. We hypothesize that this is due to the limited amount of data, large degree of averaging, and unmodeled contractile motion.

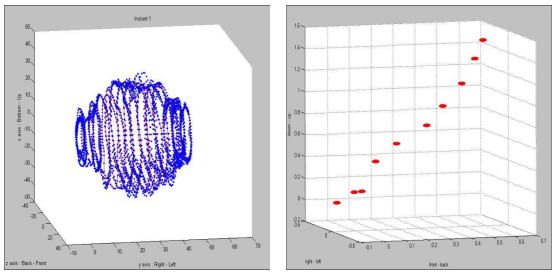

Figure 5. Left: Average heart calculated by interpolating all slices to a common phase point. Blue shows the interpolated data, red the averaged heart. Right: Trajectory of the averaged heart across 1/2 respiratory cycle

References

[1] McLeish K, Hill D, D. Atkinson JB, Razavi R. A study of the motion and deformation of the heart due to respiration. IEEE Trans on Medical Imaging 2002;21.

[2] Cootes TF, Taylor CJ. Active appearance models. In IEEE Trans. on Pattern Analysis and Machine Intelligence. Springer, 1998; 484–498.

[3] Andreopoulos A, Tsotsos J. Efficient and generalizable statistical models of shape and appearance for analysis of cardiac mri. Medical Image Analysis June 2008;12(3):335–357. ISSN 13618415.

[4] Peters TM, Linte CA, J. Moore DB, Jones DL, Guiraudon G. Towards a medical virtual reality environment for minimally invasive cardiac surgery. In MIAR, volume 5128. Springer. ISBN 978-3-540-79981-8, 2008; 1–11.

[5] Osher S, Sethian J. Fronts propagating with curvature-dependent speed: Algorithms based on hamilton-jacobi formulations. Journal of Computational Physics 1988;(79).

[6] Kohlberger T, Cremers D, Rousson M, Ramaraj R, Funka-Lea G. 4D shape priors for a level set segmentation of the left myocardium in SPECT sequences. In MICCAI, volume 4190. Springer. ISBN 3-540-44707-5, 2006; 92–100.

[7] Lynch M, Ghita O, Whelan P. Left-ventricle myocardium segmentation using a coupled level-set with a priori knowledge. Computerized Medical Imaging and Graphics 2006; 30(4):255–262. ISSN 08956111.

[8] Michael K, Witkin A, Terzopoulos D. Snakes: Active contour models. International Journal of Computer Vision January 1988;V1(4):321–331.

[9] H. J, Huang X, Metaxas DN, Axel L. Dynamic texture based heart localization and segmentation in 4-D cardiac images. In ISBI. IEEE, 2007; 852–855.

[10] Sörgel W, Vaerman V. Automatic heart localization from a 4d mri dataset. In In Proc. of SPIE Conf. on Medical Imaging. 1997; 333–344.

[11] H.G. Borgen B.M.T. Lantz RM, Mason. D. Effect of respiration on cardiac motion determined by cineangiography. Acta Radiologica Diagnosis 1977;.

[12] Pons G, Tadmor G, MacLeod R, Rosenhahn B, Brooks D. 4d cardiac segmentation of the epicardium and left ventricle. In World Cong. on Med. Physics and Bio. Eng. Munich, Germany, 2009; .

[13] K. Nehrke PB. Study of the respiratory motion of the heart using multiple navigator pulses. Proc Intl Sot Mag Reson Med 2000;(8).